molecules

MDPI

Article

Novel Co_5 and Ni_4 Metal Complexes and Ferromagnets by the Combination of 2-Pyridyl Oximes with Polycarboxylic Ligands

Foteini Dimakopoulou [1], Costantinos G. Efthymiou [1], Ciaran O'Malley [1], Andreas Kourtellaris [2], Eleni Moushi [3], Anastasios Tasiopooulos [2], Spyros P. Perlepes [4], Patrick McArdle [1], Ernesto Costa-Villén [5], Julia Mayans [5] and Constantina Papatriantafyllopoulou [1,*]

[1] School of Biological and Chemical Sciences, College of Science and Engineering, National University of Ireland Galway, University Road, H91 TK33 Galway, Ireland; f.dimakopoulou1@nuigalway.ie (F.D.); dinosef@yahoo.com (C.G.E.); c.omalley16@nuigalway.ie (C.O.); patrick.mcardle@nuigalway.ie (P.M.)
[2] Department of Chemistry, University of Cyprus, Nicosia 1678, Cyprus; kourtellaris.andreas@ucy.ac.cy (A.K.); atasio@ucy.ac.cy (A.T.)
[3] Department of Life Sciences, European University of Cyprus, Nicosia 2404, Cyprus; e.moushi@euc.ac.cy
[4] Department of Chemistry, University of Patras, 26504 Patras, Greece; perlepes@upatras.gr
[5] Departament de Química Inorgànica i Orgànica, Secció Inorgànica and Institute of Nanoscience (IN2UB) and Nanotecnology, Universitat de Barcelona, Marti i Franques 1-11, 08028 Barcelona, Spain; ernesto.costa@qi.ub.edu (E.C.-V.); julia.mayans@qi.ub.edu (J.M.)
* Correspondence: constantina.papatriantafyllopo@nuigalway.ie; Tel.: +353-91-493462

Citation: Dimakopoulou, F.; Efthymiou, C.G.; O'Malley, C.; Kourtellaris, A.; Moushi, E.; Tasiopooulos, A.; Perlepes, S.P.; McArdle, P.; Costa-Villén, E.; Mayans, J.; et al. Novel Co_5 and Ni_4 Metal Complexes and Ferromagnets by the Combination of 2-Pyridyl Oximes with Polycarboxylic Ligands. *Molecules* **2022**, *27*, 4701. https://doi.org/10.3390/molecules27154701

Academic Editors: Nikolay Gerasimchuk and Vito Lippolis

Received: 2 July 2022
Accepted: 20 July 2022
Published: 22 July 2022

Abstract: The use of 2-pyridyl oximes in metal complexes chemistry has been extensively investigated in the last few decades as a fruitful source of species with interesting magnetic properties. In this work, the initial combination of pyridine-2-amidoxime ($pyaoxH_2$) and 2-methyl pyridyl ketoxime (mpkoH) with isonicotinic acid (HINA) and 3,5-pyrazole dicarboxylic acid (H_3pdc) has provided access to three new compounds, $[Ni_4(INA)_2(pyaox)_2(pyaoxH)_2(DMF)_2]$ (**1**), $[Co_5(mpko)_6(mpkoH)_2(OMe)_2(H_2O)](ClO_4)_6$ (**2**), and $[Co_5(OH)(Hpdc)_5(H_2pdc)]$ (**3**). **1** displays a square-planar metal topology, being the first example that bears simultaneously HINA and $pyaoxH_2$ in their neutral or ionic form. The neighbouring Ni_4 units in **1** are held together through strong intermolecular hydrogen bonding interactions, forming a three-dimensional supramolecular framework. **2** and **3** are mixed-valent $Co_4^{III}Co^{II}$ and $Co_2^{III}Co^{II}_3$ compounds with a bowtie and trigonal bipyramidal metal topology, accordingly. Direct current and alternate current magnetic susceptibility studies revealed that the exchange interactions between the Ni^{II} ions in **1** are ferromagnetic (J = 1.79(4) cm^{-1}), while **2** exhibits weak AC signals in the presence of a magnetic field. The syntheses, crystal structures, and magnetic properties of **1–3** are discussed in detail.

Keywords: coordination polymers; metal complexes; carboxylates; magnetic properties; pyridyl oximes; nickel; cobalt

1. Introduction

Polynuclear metal complexes are hybrid metal–organic compounds, in which metal ions are held together through inorganic or organic ligands forming discrete species of zero dimensionality [1–4]. The synthesis and characterisation of such species have attracted an immense research interest the recent decades due to their potential applications in the environmental, biomedical, technological and industrial field [5–14]. In particular, polynuclear metal compounds often display unique structural features and combine physical properties (magnetism, luminescence, etc.) that cross the boundaries between a variety of research areas, including bioinorganic chemistry, drug discovery, catalysis, molecular magnetism, and others. In regard to the latter, the discovery that the paramagnetic metal complexes have the potential to possess magnetic properties in the absence of an

external magnetic field at very low temperature, i.e., exhibiting single molecule magnetism (SMM) behaviour, marked the commencement of a new era in the field of molecular nanomaterials [5–7]. The magnetic behaviour of SMMs results from the combination of a large ground spin state (*S*) with a large and negative easy-axis type of magnetoanisotropy as measured by the axial zero-field splitting parameter, *D*. Such species often display extraordinary properties at the nanoscale level, e.g., quantum tunnelling of magnetisation and quantum phase interference, and they are excellent candidates in data storage devices applications, quantum computers, imaging, etc. [15–20]. On the other hand, metal complexes with small magnetic anisotropy have the potential to be used as magnetic refrigerants in magnetic refrigeration, which is an environmentally friendly technique for refrigeration at ultra-low temperatures [8–10].

The connection of metal complexes through polytopic organic linkers leads to the formation of coordination polymers. In the case of 1D coordination polymers consisting of paramagnetic building units, strong exchange interactions might be present along the chain, which gives rise to another family of magnetic materials, namely single-chain magnets (SCMs) [21–23]. SCMs are excellent candidates for applications similar to those of SMMs; furthermore, they have been investigated as molecular ferromagnets, synthetic metallic conductors, non-linear optical or ferroelectric materials [24–26]. As the dimensionality of the network increases, the accessible porosity of the material increases too, leading to porous coordination polymers known as metal–organic frameworks (MOFs) [27–29]. MOFs are of special interest as they display appealing structural features, such as large surface area and tuneable porosity, which make them suitable for the adsorption of large guest molecules. The porosity is often combined with magnetism and/or another physical property, e.g., photoluminescence, etc. The synergistic effect between different properties may enhance the performance of such species in applications related to sensing, catalysis, drug delivery, spintronics, photonics, etc. [30–37].

The structural and physical properties of the discrete metal complexes and coordination polymers are strongly affected by the nature of the metal ion(s) and the ligand(s) present in their structures. The organic linkers possess suitable sites for metal coordination, and they provide the desirable stability through the formation of hydrogen bonding, π–π stacking, and other intermolecular interactions. Such interactions are significant, and they are even more profound when metal complexes are linked to form coordination polymers or MOFs, as they can introduce structural flexibility and affect the MOF selectivity toward specific guest molecules [38]. One family of ligands that has been intensively explored for the synthesis of metal compounds with interesting magnetic properties is the 2-pyridyl oximes; 2-pyridyl oximes have the general formula (py)C(R)NOH (Scheme 1), with the electronic properties and functionality of the R group playing a crucial role on the coordination properties of the ligands. (py)C(R)NOH have been key "players" in several areas of single-molecule and single-chain magnetism, as they tend to link a large number of metal ions, favouring also the presence of ferromagnetic exchange interactions between the metal centres [39–49]. Although the employment of 2-pyridyl oximes has led to significant breakthroughs in the areas of molecular magnetism, their use in the field of MOFs remains limited. To this end, our group has been investigating the ligand blend 2-pyridyl oximes (e.g., pyridine-2-amidoxime and 2-methyl pyridyl ketoxime) and polycarboxylates, which has led to the isolation of the first 2-pyridyl oxime-based MOFs, and several coordination polymers [50–52]. Some of the MOFs display unprecedented metal topologies and metal ion encapsulation capability. A representative such example is $[Cu_4(OH)_2(pma)(mpko)_2]_n$, pma^{4-} = the tetra-anion of 1,2,4,5-benzene tetracarboxylic acid, and $mpko^-$ = the anionic form of 2-methyl pyridyl ketoxime, which exhibits a good Fe^{III} adsorption capacity; interestingly, the magnetic properties of the latter are strongly related to the amount of the encapsulated Fe^{III} ions [52].

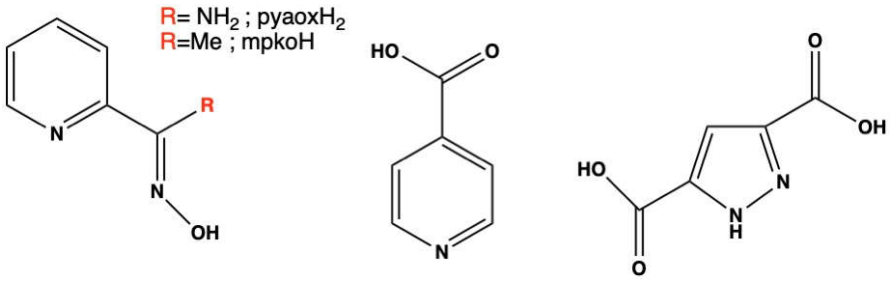

Scheme 1. Schematic representation of 2-pyridyl oximes (left), isonicotinic acid (centre) and 3,5-pyrazole dicarboxylic acid (right).

With the above in mind, we decided to explore further the reaction mixture of 2-pyridyl oximes and polycarboxylic acids, and, in particular, we introduced isonicotinic acid (pyridine-4-carboxylic acid) [53–65] and 3,5-pyrazole dicarboxylic acid [66–85] to the reaction system (Scheme 1). Both carboxylic acids have been extensively investigated in the field of coordination compounds, and they have been proven a fruitful source of discrete metal complexes and coordination polymers; [53–85] yet their combination with oximic ligands remains unexplored. Herein, we report three new Ni_4 (**1**), $Co^{III}_4Co^{II}$ (**2**), and $Co^{III}_2Co^{II}_3$ (**3**) complexes from this ligand combination. The syntheses, crystal structures and magnetic properties of these compounds have been studied, revealing that **1** is a ferromagnet being the first example bearing both $pyaoxH_2$ and HINA. **3** displays an unprecedented $\{Co^{II}_3(\mu_3\text{-}OH)\}^{7+}$ planar unit which can be used as a model for the study of spin frustration in triangular Co^{II}_3 systems.

2. Results and Discussion

2.1. Synthetic Discussion

Our group has been exploring the employment of 2-pyridyl oximes in combination with polycarboxylic acids toward the synthesis of new metal compounds. The latter involved experiments with the use of benzene-1,4-dicarboxylic acid, benzene-1,3,5-tricarboxylic acid and benzene-1,2,4,5-tetracarboxylic acid [50–52]. The initial promising results prompted us to explore further this reaction system by using different carboxylic ligands, such as isonicotinic acid (HINA) and 3,5-pyrazole dicarboxylic acid (H_3pdc). To this end, a wide range of experiments was conducted, aiming at studying the effect of different synthetic parameters (temperature, presence/absence or kind of base, metal ratio of the reactants, metal sources, etc.) on the identity and crystallinity of the isolated product(s) and the yield of the reaction.

The reaction mixture of $Ni(ClO_4)_2.6H_2O$/$pyaoxH_2$/HINA (2:4:1.5) in DMF at 110 °C gave a dark brown solution from which dark brown crystals of $[Ni_4(INA)_2(pyaox)_2(pyaoxH)_2(DMF)_2]$ (**1**) were subsequently isolated in good yield. The stoichiometric equation of the reaction that led to the formation of **1** is represented in Equation (1).

$$4Ni(ClO_4)_2.6H_2O + 4pyaoxH_2 + 2HINA + 2DMF + 8Et_3N \xrightarrow{DMF} \underset{\mathbf{1}}{[Ni_4(INA)_2(pyaox)_2(pyaoxH)_2(DMF)_2]} + 8ClO_4^- + 8HNEt_3^+ + 24H_2O \quad (1)$$

The kind of base and/or metal source does not have any impact on the identity of the isolated compound, but it affects its crystallinity. The next step included the replacement of Ni^{II} by $Co^{II/III}$ wishing to shed light on how the type of the metal ion affects the identity of the product. Similar reactions that led to **1** were performed by using a Co^{II} source instead of Ni, which, in their vast majority, led to the isolation of previously reported single-ligand Co^{II} MOFs based on INA^- [53,54]. Likewise, the use of mpkoH instead of $pyaoxH_2$ provided access to compounds that contain INA^-. This prompted us to perform reactions

with an excess of the oximic ligand, which led to the new mixed-valent cationic pentanuclear compound $[Co^{III}_4Co^{II}(mpko)_6(mpkoH)_2(OMe)_2(H_2O)](ClO_4)_6$ (**2**), while the use of H_3pdc in the place of HINA led to the isolation of the new neutral pentanuclear compound $[Co_5(OH)(Hpdc)_5(H_2pdc)]$ (**3**). The stoichiometric equations of the reaction that describe the formation of **2** and **3** are shown in Equations (2) and (3).

$$5Co(ClO_4)_2.6H_2O + 8mpkoH + O_2 + 4NaO_2CMe + 2MeOH \longrightarrow$$

$$[Co_5(mpko)_6(mpkoH)_2(OMe)_2(H_2O)](ClO_4)_6 + 4Na^+ + 4ClO_4^- + 4MeCO_2H + 31H_2O \quad (2)$$

2

$$5Co(O_2CMe)_2.4H_2O + 6H_3bdc + 1/2O_2 + 10Et_3N \xrightarrow{DMF}$$
$$[Co_5(OH)(Hpdc)_5(H_2pdc)] + 10HNEt_3^+ + 10MeCO_2^- + 20H_2O \quad (3)$$

3

2.2. Description of Structures

Representations of the molecular structures of **1–3** are shown in Figures 1–3. Selected interatomic distances and angles are listed in Tables S1–S3.

1 crystallizes in the monoclinic space group $P2_1/c$. Its structure is based on neutral, centrosymmetric $[Ni_4(INA)_2(pyaox)_2(pyaoxH)_2(DMF)_2]$ units (Figure 1) that are held together through strong hydrogen bonding interactions forming a 3D network (Figure S1). The Ni_4 compound in **1** is composed of two distorted octahedral (Ni1 and its symmetry equivalent) and two square planar Ni^{II} atoms (Ni2 and its symmetry equivalent), which are connected through two $\eta^1{:}\eta^1{:}\eta^1{:}\mu$ $pyaoxH^-$, and two $\eta^1{:}\eta^1{:}\eta^1{:}\eta^2{:}\mu_3$ $pyaox^{2-}$ ligands (Scheme 2). The coordination sphere in Ni1 and Ni1′ is completed by one terminally ligated DMF molecule and one monodentate INA^- ion. The four metal centres in **1** are coplanar.

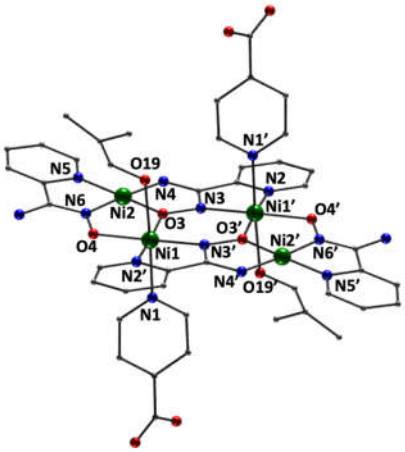

Figure 1. Representation of the molecular structure of **1**. Colour code: Ni, green; N, blue; O, red; C, grey.

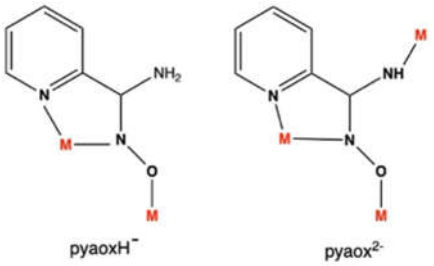

Scheme 2. The coordination modes of the $pyaox^{2-}$ and $pyaoxH^{-}$ ligands in **1**.

The carboxylate group of the deprotonated INA^{-} ligand forms strong intermolecular hydrogen bonding interactions with the neutral and/or deprotonated amino groups from neighbouring Ni_4 species: (N7···O1 = 2.848 Å, H7B···O1 = 2.029 Å, N7-H7B···O1 = 158.92°; N7···O2 = 3.005 Å, H7A···O2 = 2.197 Å, N7-H7A···O2 = 156.46°; N4···O1 = 3.053 Å, H1N4···O1 = 2.186 Å, N4-H1N4···O1 = 171.52°). These intermolecular interactions along with the fact that that neighbouring Ni_4 units are in close proximity (Ni1 … Ni2 = 7.7 Å) result in the formation of a three-dimensional supramolecular network. The N7-H7A···O2 and N4-H1···O1 H-bonds favour the formation of a 2D supramolecular network (Figure S2), whereas the Ni_4 complexes lie roughly on the same plane and each complex is surrounded by six neighbouring Ni_4 units in a hexagonal topological arrangement. Neighbouring 2D planes are arranged in a parallel fashion, being interconnected through the N7-H7B···O1 H-bond, leading to the formation of a 3D supramolecular network (Figure 1, right), which can be described as a pseudo 3D polymer or as a 3D supramolecular framework. It is worth mentioning that **1** displays significant thermal stability (Figure S3), which is a result of its pseudo-polymeric nature. In particular, there is a mass loss of ca 2% below 100 °C, which can be attributed to adsorbed humidity; this is then followed by a plateau with the step at 350 °C corresponding to the compound breakdown.

The tetranuclear $\{Ni_4\}$ single-decker core of compound **1** has been found previously as a fundamental building unit in a couple of multiple-decker based polynuclear Ni complexes. Being composed by three and four $\{Ni_4\}$ layers/deckers, respectively, Ni_{12} and Ni_{16} complexes can be assumed as the trimer and the tetramer version of **1** [40,41]. Both Ni_{12} and Ni_{16} are ferromagnets bearing a high-spin ground state of S = 6 and S = 8, respectively. Ferromagnets are a special category of magnetic materials with their properties being derived by the ferromagnetic exchange coupling among the paramagnetic centres. They are candidates for interesting potential applications, such as spintronics, magnetic coolers, etc.

2 crystallizes in the triclinic space group $P\bar{1}$. Its structure consists of $[Co^{II}Co^{III}_4(mpko)_6(mpkoH)_2(OMe)_2(H_2O)]$ metal complexes and ClO_4^- counterions (Figure 2). The five metal ions are held together through four $\eta^1{:}\eta^1{:}\eta^1{:}\mu$ $mpko^-$ and two $\eta^2{:}\eta^1{:}\eta^1{:}\mu_3$ $mpko^-$ ions, forming a distorted bowtie topology. Furthermore, two μ-MeO- ions bridge the Co^{III} ions, i.e., Co3 and Co5, and Co1 and Co4, respectively. Alternatively, the structure of **2** can be described as consisting of a central $\{Co^{II}(mpko)_4(H_2O)\}^{2+}$ unit on both sides of which are located two dinuclear $\{Co^{III}_2(mpko)_3(mpkoH)\}^{3+}$ moieties.

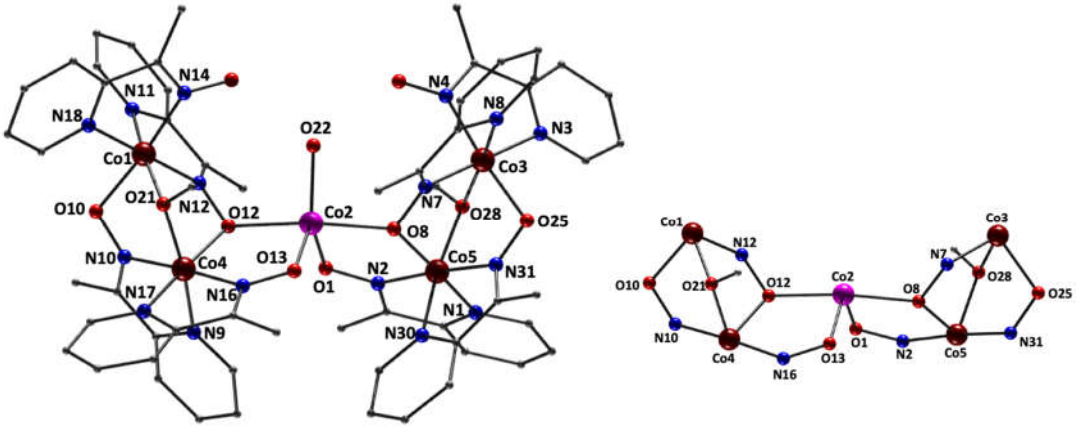

Figure 2. Representation of the molecular structure of **2** (**left**) and the bowtie metal topology of its structural core (**right**). Colour code: Co^{II}, pink; Co^{III}, dark red; N, blue; O, red; C, grey.

Co1 and Co3–Co5 are six-coordinate with an octahedral coordination geometry. Co2 is five-coordinate displaying trigonal bipyramidal geometry (τ = 0.77) [86]. The coordination spheres of Co1 and Co3 are completed by two neutral chelate mpkoH ligands, while one terminally ligated H_2O molecule completes the coordination sphere of Co2. The Co_5 cations in **2** are in proximity with the shortest metal···metal distance between the neighbouring Co_5 units being 6.537 Å (Co3···Co5). The crystal structure of **2** is stabilised through strong intramolecular hydrogen bonding interactions between the terminally ligated water molecule (O22, donor) and the oximic groups (O6, O15), which act as acceptors: O22···O6 = 2.589 Å, H6···O22 = 2.041 Å, O6-H6···O22 = 123.75°; O22···O2 = 2.644 Å, H2···O22 = 2.052 Å, O2-H2···O22 = 128.87

3 crystallizes in the monoclinic space group I2/a consisting of mixed-valent pentanuclear compounds $[Co^{III}_2Co^{II}_3(OH)(Hpdc)_5(H_2pdc)]$ (Figure 3, left). The five metal centres in **3** are held together through a μ_3-OH- ion and six $\eta^1{:}\eta^1{:}\eta^1{:}\eta^1{:}\mu$ carboxylate ligands. The former link Co2, Co3 and Co5, forming a plane above and below of which the remaining two metal ions are located; hence, the structural core of **3** possesses a trigonal bipyramidal metal topology with the distance of Co1 and Co4 from the equatorial plane being 3.848 Å and 3.896 Å, correspondingly (Figure 3, right).

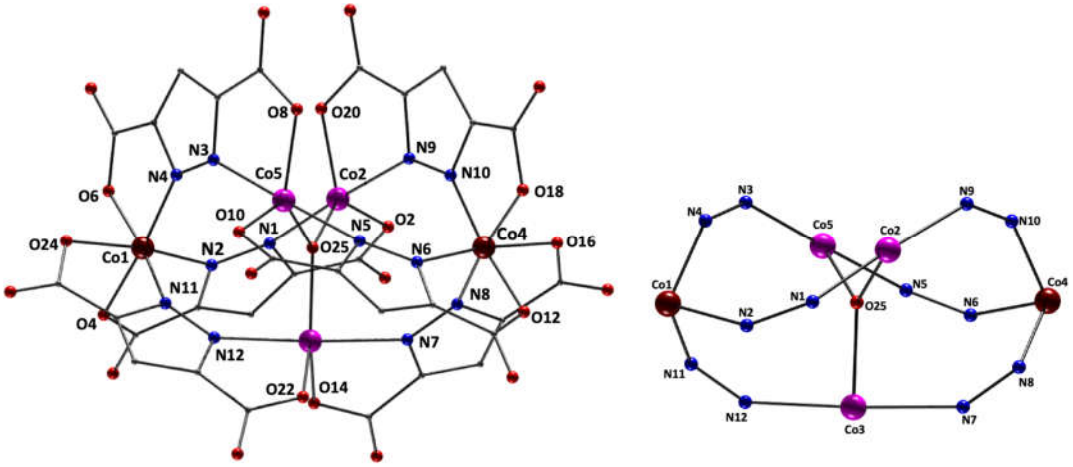

Figure 3. Representation of the molecular structure of **3** (**left**) and the trigonal pipyramidal metal topology of its structural core (**right**). Colour code: Co^{II}, pink.; Co^{III}, dark red; N, blue; O, red; C, grey.

Co1 and Co4 are six-coordinate with an octahedral coordination geometry. Co2, Co3 and Co5 are five coordinate displaying trigonal bipyramidal geometry (τ = Co2, 0.83; Co3, 0.76; Co5, 0.77) [86]. The Co_5 molecules in **3** are relatively in close proximity with the shortest metal···metal separation between the adjacent Co_5 units being 7.937 Å (Co4···Co4). **3** is the first example of a Co compound bearing H_3pdc in its neutral or anionic form, being also one of the highest nuclearity discrete metal complexes with this ligand.

2.3. Magnetism Studies

Direct current magnetic susceptibility measurements (DC) were carried out on samples of **1**, **2** and **3** in the 2–300 K temperature range and under a field of 0.03 T (1.28 MHz), and they are plotted as $\chi_M T$ vs. T plot. (Figure 4). The $\chi_M T$ values at room temperature (2.30, 1.95 and 4.31 $cm^3\ mol^{-1}\ K$ for **1**, **2** and **3**, respectively) are very close to the theoretical spin-only value of 2.00, 1.875 and 5.625 $cm^3\ mol^{-1}\ K$ corresponding to two Ni^{II}, one Co^{II} and three Co^{II} non-interacting cations, respectively.

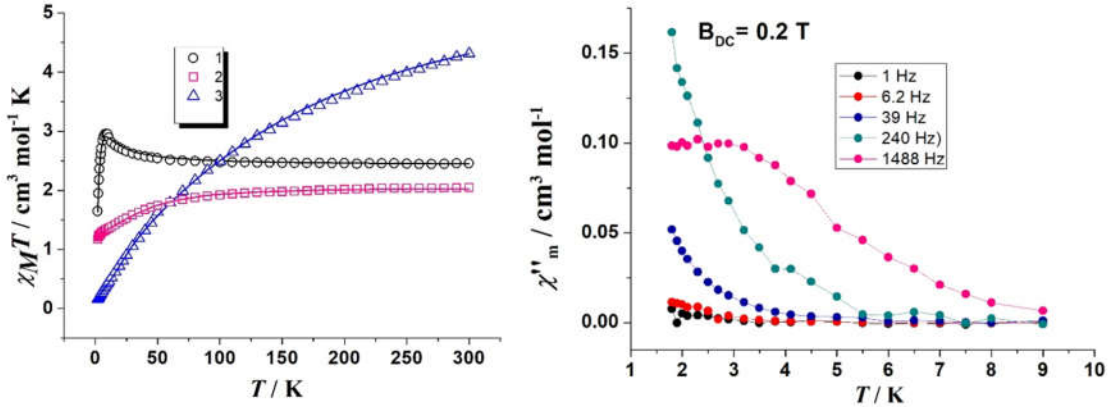

Figure 4. (**Left**) $\chi_M T$ vs. T plots for complexes **1** (black circles), **2** (pink squares) and **3** (blue triangles). Solid line represents the best fit. (**right**) χ_M″ vs. T plot for complex **2** at different frequencies under a dc field of 0.2 T.

Complex **1** is a tetranuclar Ni^{II} system, in which Ni2 and Ni2′ present a square-planar geometry being diamagnetic, hence, magnetically, the molecule behaves as a dinuclear Ni^{II} complex. The $\chi_M T$ vs. T curve for **1** shows a weak ferromagnetic interaction between the Ni^{II} paramagnetic cations, reaching a value of 2.96 cm^3 mol^{-1} K at 9 K; then, there is an abrupt decay until it reaches to a minimum value of 1.64 cm^3 mol^{-1}K at 2 K, due to weak intermolecular interactions or anisotropy effects. The curve has been fitted using the Hamiltonian $\hat{H} = -2J\ (S_{Ni1} \cdot S_{Ni1'}) + DS_z + \Sigma\mu g_{eff} HS$ yielding in the best fitting values of J = 1.79(4) cm^{-1}, D_{ion} = 2.48(2) cm^{-1} and g = 2.20 using PHI software [87]. This is in perfect agreement with previously reported multiple decker Ni complexes based on Ni_4 layers that exhibit similar magnetic exchange pathways [40,41].

Complex **2** is a pentanuclear Co compound with only one paramagnetic Co^{II} being present in the molecule; thus, it behaves as a mononuclear compound. The $\chi_M T$ decay when lowering temperature is due to the axial zero field splitting of the Co^{II} cation evaluated as D_{ion} = 47.7(7) cm^{-1} and g = 2.085(2). The relatively high value of D parameter agrees with the trigonal bipyramid distorted environment. Alternate-current (AC) measurements were performed in the 1–1488 Hz frequency range, and weak tails were observed (Figure 4, right) in the presence of a magnetic field of 0.2 T, which is indicative of the single-ion magnetism behaviour for **2**. However, this AC response is too weak to extract any relaxation parameter.

Complex **3** possesses an uncommon magnetic core: usually, μ_3-OR cobalt trimers present a defective-cubane topology, whereas **3** is a μ_3-O tricobalt complex where the oxo donor and the three cobalt atoms are co-planar, defining a triangular arrangement of cations with the three Co-O-Co bond angles being very similar (~120°). A CCDC search does not reveal any similar structure for which the magnetic study has been performed, and it makes complex **3** a quite interesting study case for the spin-frustrated Co^{II} triangle. The $\chi_M T$ curve for **3** reveals an antiferromagnetic coupling between the three Co^{II} cations; it continuously decreases with decreasing temperature until it reaches the value of 0.200 cm^3 mol^{-1} K at 2 K. The used Hamiltonian was $\hat{H} = -2J\ (S_{Co2} \cdot S_{Co3} + S_{Co3} \cdot S_{Co5} + S_{Co2} \cdot S_{Co5}) + DS_z + \Sigma\mu g_{eff} HS$, yielding in the fitting parameters J = −14.18(1) cm^{-1}, g = 2.075(3) and D = 10.55(4) cm^{-1}.

3. Materials and Methods

3.1. Materials, Physical, and Spectroscopic Measurements

All the manipulations were performed under aerobic conditions using materials (reagent grade) and solvents as received. Nickel(II) perchlorate hexahydrate (CAS: 13520-61-1), Isonicotinic acid 99% (CAS: 55-22-1), 3,5 pyrazole dicarboxylic acid monohydrate 97%

(CAS: 303180-11-2), Cobalt(II) acetate tetrahydrate 98% A.C.S.(CAS: 6147-53-1) and cobalt(II) chloride hexahydrate 98% (CAS: 7791-13-1) were obtained as received from Sigma-Aldrich. Dimethylformamide >99.5% HPLC grade (68-12-2) was purchased from Fluka and triethylamine (CAS: 121-44-8) was obtained from Sigma-Aldrich. mpkoH and pyaoxH_2 was prepared as described elsewhere [88,89]. WARNING: *Perchlorate salts are potentially explosive; such compounds should be used in small quantities and treated with utmost care at all times*.

Elemental analysis (C, H, N) was performed by the in-house facilities of the National University of Ireland Galway, School of Chemistry. Solvothermal synthesis was performed in a Binder oven. IR spectra (4000–400 cm^{-1}) were recorded on a Perkin-Elmer Spectrum 400 FT-IR spectrometer. Powder X-ray diffraction was performed with an INEL X-ray diffractometer EQUINOX 0000 using Cu K_a radiation (λ = 1.54178 Å, 35 kV, 25 mA).. Thermogravimetric analysis (TGA) and differential scanning calorimetry (DSC) were carried out in open aluminium crucibles using an STA625 thermal analyzer (Rheometric Scientific, Piscataway, NJ, USA) with nitrogen being purged in ambient mode. Solid-state, variable-temperature and variable-field magnetic data were collected on single crystals of each sample using an MPMS5 Quantum Design magnetometer operating at 0.03 T in the 300–2.0 K range for the magnetic susceptibility and at 2.0 K in the 0–5 T range for the magnetization measurements. Diamagnetic corrections were applied to the observed susceptibilities using Pascal's constants.

3.2. Compound Synthesis

3.2.1. Synthesis of [Ni_4(INA)$_2$(pyaox)$_2$(pyaoxH)$_2$(DMF)$_2$] (**1**)

$Ni(ClO_4)_2.6H_2O$ (0.073 g, 0.20 mmol) and Et_3N (114 µL, 0.80 mmol) were added in 5 mL of pyaoxH_2 (0.054 g, 0.40 mmol) in DMF in a glass vial with a plastic lid. The resultant solution was put in an oven and heated at 110 °C for 1 h during which time the colour of the solution turned dark brown. Then, 5 mL of HINA (0.018 g, 0.15 mmol) were added, and the vial was placed in the oven for a further 48 h. After 2 days, X-ray quality dark red, block-shaped crystals of **1** were observed. The crystals were collected by filtration, washed with DMF and acetone and dried in air. Yield 43%. Anal. Calc. for **1**: C, 43.13; H, 3.96; N, 19.16 Found: C, 43.87; H, 4.01; N, 19.41%. IR data, Figure S3: ν (cm^{-1}) = 3299 d, 3155 d, 1648 sh, 1600 sh, 1584, 1548 s, 1479 s, 1455 w, 1412 s, 1381 w, 1355 s, 1313 w, 1304 w, 1276 w, 1262 w, 1231 w, 1213 w, 1181 m, 1155 m, 1132 w, 1098 m, 1058 m, 1027 m, 1018 m, 953 m, 864 m, 833 w, 801 m, 781 s, 762 w, 750 w, 731 w, 707 m, 681 s, 669 m, 657 w.

3.2.2. Synthesis of [Co_5(mpko)$_6$(mpkoH)$_2$(OMe)$_2$(H_2O)](ClO_4)$_6$ (**2**)

Sodium acetate trihydrate (0.027 g, 0.2 mmol) and 2-pyridyl ketoxime (0.027 g, 0.2 mmol) were dissolved in 15 mL MeOH in a glass vial with a plastic lid. The solution was stirred on a hot plate for 10 min. $Co(ClO_4)_2.xH_2O$ (0.073 g, 0.2 mmol) was then added and the solution turned dark red; it was left under stirring for 30 min further after which it was filtered. The solution was left in an open vial for slow evaporation, and after 2 days, dark red X-ray quality single crystals were observed. Yield 45%. Anal. Calc. for **2**: C, 36.86; H, 3.98; N, 7.68% Found: C, 36.52; H, 4.23; N, 7.16%. IR data, Figure S4: ν (cm^{-1}) = 3532 w, 3420 w, 3146 w, 3060 w, 3000 w, 1750 w, 1752 w, 1632 w, 1602 s, 1575 w, 1528 s, 1475 s, 1440 s, 1379 w, 1302 w, 1263 w, 1185 s, 1074 s, 1028 w, 992 w, 931 w, 883 w, 822 w, 774 s, 749 m, 695 s, 655 m.

3.2.3. Synthesis of [Co_5(OH)(Hpdc)$_5$(H_2pdc)] (**3**)

Method A: H_3pdc (0.034 g, 0.20 mmol), pyaoxH_2 (0.054 g, 0.40 mmol) and Et_3N (10 µL mL, 0.07 mmol) were dissolved in 5 mL of DMF in a glass vial with a plastic lid. $Co(CH_3COO)_2.4H_2O$ (0.024 g, 0.10 mmol) was added, and the vial was placed in the oven at 110 °C for 24 h, after which the solution turned brown–pink and X-

ray quality purple needles of 2 were formed. The crystals were collected by filtration, washed with DMF and acetone and dried in air. Yield 90%. Anal. Calc. for **3**: C, 29.13; H, 1.14; N, 13.59%. Found: C, 28.74 H, 1.19; N, 13.29%. IR data: ν (cm^{-1}) = 3544 w, 3421 w, 3124 w, 3040 w, 2791 w, 2476 w, 1622 s, 1602 s, 1494 m,1468 m,1438 w,1412 w, 1371 s, 1306 s, 1259 s, 1097 w, 1059 m,1011 s, 888 w, 841 s, 815 m, 802 w, 777 s, 662 w.

Method B: Method A was followed with the only difference being the omission of $pyaoxH_2$ from the reaction mixture. The sealed vial was placed in the oven at 110 °C, and after one day, crystalline purple needles of 2 were observed. Yield: 80%

Method C: Method A was repeated but using $CoCl_2.6H_2O$ (0.023 g, 0.10 mmol) instead of $Co(CH_3COO)_2.4H_2O$. The vial was left in the oven at 110 °C, and after one day, crystalline purple needles of 2 were observed. Yield: 90%. The product in Methods B and C was identified as **2** by IR spectral comparison with material obtained in method A (Figure S5) and unit cell determination.

3.3. Single-Crystal X-Ray Crystallography

Single-crystal diffraction data for **1** were collected in an Oxford Diffraction Xcalibur CCD diffractometer using graphite-monochromatic Mo-Kα radiation (λ = 0.71073 Å) at room temperature. Single-crystal diffraction data for **2** and **3** were collected in an Oxford-Diffraction SuperNova diffractometer equipped with a CCD area detector and a graphite monochromator utilising Mo-Kα (for **2**) and Cu-Kα radiation (for **3**). The structures were solved using SHELXT and [90] embedded in the OSCAIL software [91]. The non-H atoms were treated anisotropically, whereas the hydrogen atoms were placed in calculated, ideal positions and refined as riding on their respective carbon atoms. Molecular graphics were produced with DIAMOND [92]. We note that crystal twining occurs in **2**, which affects the quality of the structure. We carried out many experiments in order to grow single crystals of better quality; however, this has not been achieved. We collected three sets of data using two different diffractometers and used the best set to solve the structure.

Unit cell data and structure refinement details are listed in Table 1. The crystal structures have been deposited with the Cambridge Crystallographic Data Centre (CCDC 2180525-2180527), and they can be accessed, free of charge, by filling out the application form at https://www.ccdc.cam.ac.uk/structures/.

Table 1. Crystallographic data for complexes **1–3.**

Complex	**1**	**2**	**3**
Empirical formula	$C_{44}H_{44}N_{14}Ni_4O_{10}$	$C_{116}H_{128}Cl_9Co_{10}N_{32}O_{60}$	$C_{30}H_6Co_5N_{12}O_{25}$
Formula weight	1163.77	3838.85	1229.12
Crystal system	Monoclinic	Triclinic	Monoclinic
Space group	*P*2$_1$/*c*	*P*-1	*I*2/*a*
a (Å)	11.6069(5)	11.28230(10)	19.1464(8)
b (Å)	12.4541(5)	15.2083(2)	29.8272(10)
c (Å)	18.1577(9)	23.9909(4)	23.4279(7)
α (°)	90	84.1200(10)	90
β (°)	107.901(5)	86.0130(10)	92.567(3)
γ (°)	90	88.3410(10)	90
V (Å^3)	2497.7(2)	4083.91(9)	13365.9(8)
Z	2	1	8
ρ_{calc} (g cm^{-3})	1.547	1.561	1.222
μ (mm^{-1})	1.554	1.229	1.014
Measd/independent reflns (R_{int})	4549/3473 (0.0492)	14336/11846 (0.0301)	11879/6538 (0.0431)
Parameters refined	326	1020	649

GoF (on F^2)	0.981	1.041	0.956
R_1 [a] ($I > 2\sigma(I)$)	0.0453	0.0939	0.0818
wR_2 [b] ($I > 2\sigma(I)$)	0.1181	0.2691	0.2478
$(\Delta\rho)_{max}/(\Delta\rho)_{min}$ (e Å^{-3})	0.644/−0.788	3.867/−2.563	0.715/−0.374

[a] $R_1 = \Sigma(||F_o| - |F_c||)/\Sigma(|F_o|)$. [b] $wR_2 = \{\Sigma[w(F_o^2-F_c^2)^2]/\Sigma[w(F_o^2)^2]\}^{1/2}$.

4. Conclusions

The combination of 2-pyridyl oximes (pyridine-2 amidoxime, H_2pyaox; 2-methyl pyridyl ketoxime, Hmpko) with isonicotinic acid (HINA) and 3,5-pyrazole dicarboxylic acid (H_3pdc) provided access to three new Ni^{II} and $Co^{II/III}$ metal complexes. Among them, $[Ni_4(INA)_2(pyaox)_2(pyaoxH)_2(DMF)_2$ (**1**) is a planar centrosymmetric tetranuclear compound that can be characterised as a pseudo-polymer due to the strong hydrogen bonding interactions between the neighbouring discrete units. It is the first reported metal compound that bears both $pyaoxH_2$ and HINA in their neutral or anionic form. **2** is a pentanuclear $Co^{III}_4Co^{II}$ complex with a bowtie topology, while **3** is a $Co^{III}_2Co^{II}_3$ complex with a trigonal bipyramidal metal topology. The three Co^{II} cations in **3** are co-planar with the bridging μ_3-OH- ion providing a unique spin frustration model for triangular Co^{II}_3 systems.

The magnetic properties of **1–3** have been studied and revealed that there are ferromagnetic interactions between the two paramagnetic Ni^{II} ions in **1** (J = 1.79(4) cm^{-1}), which is in accordance with previously reported multiple decker Ni_{12} and Ni_{16} compounds based on Ni_4 repeating units [40,41]. **2** displays weak AC signals in the presence of a magnetic field, while in the case of **3,** the dominant exchange interactions between the metal ions are antiferromagnetic. **3** is a unique example of a OH-centred triangular Co^{II}_3 system in which all the Co atoms and the OH^- are co-planar; hence, it is an interesting case study for spin frustration.

Although the isolation of a compound that contains both a 2-pyridyl oxime and isonicotinic acid (HINA) has been successfully achieved in the case of **1**, this has not been the case for 3,5-pyrazole dicarboxylic acid (H_3pdc). Further studies that include the optimisation of the reaction conditions that will favour the presence of both ligands in the same metal complex, e.g., full deprotonation of ligands, nature of metal ion, etc., are currently in progress and will be reported in the near future.

Supplementary Materials: The following are available online at www.mdpi.com/article/10.3390/molecules27154701/s1, Table S1. Selected interatomic distances (Å) and angles for **1**; Table S2. Selected interatomic distances (Å) and angles for **2**; Table S3. Selected interatomic distances (Å) and angles for **3**; Figure S1. The 2D supramolecular network in **1** coming from the arrangement of Ni4 clusters through H-bonding interactions (left), and the arrangement of two parallel 2D supramolecular planes (right); Figure S2. TGA-DTG (top) and DSC curves (bottom) of compound **1**; Figure S3. IR spectrum of compound **1**; Figure S4. IR spectrum of compound **2**; Figure S5. IR spectra of compound **3**: crystals from method A, top; crystals from method B, middle; crystals from Method C, bottom; Figure S6. Powder XRD patterns of compound **1**: experimental powder pattern, top; simulated, bottom.

Author Contributions: F.D. performed the synthesis, crystallisation and preliminary characterisation of compounds **1** and **3**. C.G.E./S.P.P. performed the synthesis, crystallisation and preliminary characterisation of compound **2**. C.O.M./P.M.A. collected crystallographic data, solved and refined the crystal structure of **1**. A.K./E.M./A.T. collected crystallographic data, solved and refined the crystal structures of **2** and **3**. J.M./E.C.-V. performed the magnetic measurements, interpreted the results and wrote the relevant part of the paper. C.P. coordinated the research and wrote the paper based on the reports of her collaborators. All authors have read and agreed to the published version of the manuscript.

Funding: This research was funded by the National University of Ireland Galway with a Hardiman Scholarship to F.D.

Data Availability Statement: Not available.

Conflicts of Interest: The authors declare no conflict of interest.

Sample Availability: Not available.

References

1. Papatriantafyllopoulou, C.; Moushi, E.; Christou, G.; Tasiopoulos, A.J. Filling the gap between the quantum and classical worlds of nanoscale magnetism: Giant molecular aggregates based on paramagnetic 3d metal ions. *J. Chem. Soc. Rev.* **2016**, *45*, 1597.
2. Kostakis, G.E.; Perlepes, S.P.; Blatov, V.; Proserpio, D.M.; Powell, A.K. High-nuclearity cobalt coordination clusters: Synthetic, topological and magnetic aspects. *Co-ord. Chem. Rev.* **2012**, *256*, 1246.
3. Bagai, R.; Christou, G. The Drosophila of single-molecule magnetism: [Mn12O12(O2CR)16(H2O)4]. *Chem. Soc. Rev.* **2009**, *38*, 1011.
4. Mitchell, K.J.; Abboud, K.A.; Christou, G. Atomically-precise colloidal nanoparticles of cerium dioxide. *Nat. Commun.* **2017**, *8*, 1445.
5. Schmitt, W.; Murugesu, M.; Goodwin, J.C.; Hill, J.P.; Mandel, A.; Bhalla, R.; Anson, C.E.; Heath, S.L.; Powell, A.K. Strategies for producing cluster-based magnetic arrays. *Polyhedron* **2001**, *20*, 1687.
6. Christou, G.; Gatteschi, D.; Hendrickson, D.N.; Sessoli, R. Single-molecule magnets. *MRS Bull.* **2000**, *25*, 66.
7. Gatteschi, D.; Sessoli, R. Quantum tunneling of magnetization and related phenomena in molecular materials. *Angew. Chem. Int. Ed.* **2003**, *42*, 268.
8. Peng, J.-B.; Zhang, Q.-C.; Kong, X.-J.; Ren, Y.-P.; Long, L.-S.; Huang, R.-B.; Zheng, L.-S.; Zheng, Z. A 48-Metal Cluster Exhibiting a Large Magnetocaloric Effect. *Angew. Chem. Int. Ed*. **2011**, *123*, 10837.
9. Theil, E.C.; Behera, R.K.; Tosha, T. Ferritins for chemistry and for life. *Coord. Chem. Rev.* **2013**, *257*, 579.
10. Sauer, K.; Yano, J.; Yachandra, V.K. X-ray spectroscopy of the photosynthetic oxygen-evolving complex. *Coord. Chem. Rev.* **2008**, *252*, 318.
11. Leng, J.-D.; Liu, J.-L.; Tong, M.-L. Unique nanoscale $\{Cu^{II}_{36}\ Ln^{III}_{24}\}$(Ln= Dy and Gd) metallo-rings. *Chem. Commun.* **2012**, *48*, 5286.
12. Loll, B.; Kern, J.; Saenger, W.; Zouni, A.; Biesiadka, J. Towards complete cofactor arrangement in the 3.0 Å resolution structure of photosystem II. *Nature* **2005,** *438*, 1040.
13. Taft, K.L.; Papaefthymiou, G.C.; Lippard, S.J. A mixed-valent polyiron oxo complex that models the biomineralization of the ferritin core. *Science* **1993**, *259*, 1302.
14. Zhang, Z.-M.; Pan, L.-Y.; Lin, W.-Q.; Leng, J.-D.; Guo, F.-S.; Chen, Y.-C.; Liu, J.-L.; Tong, M.-L. Wheel-shaped nanoscale 3d–4f {Co II 16 Ln III 24} clusters (Ln = Dy and Gd). *Chem. Commun.* **2013**, *49*, 8081.
15. Wernsdorfer, W.; Chakov, N.E.; Christou, G. Quantum phase interference and spin-parity in Mn 12 single-molecule magnets. *Phys. Rev. Lett.* **2005**, *95*, 037203.
16. Adams, S.T.; da Silva Neto, E.H.; Datta, S.; Ware, J.F.; Lampropoulos, C.; Christou, G.; Myaesoedov, Y.; Zeldov, E.; Friedman, J.R. Geometric-Phase Interference in a Mn 12 Single-Molecule Magnet with Truly Fourfold Rotational Symmetry. *Phys. Rev. Let.* **2013**, *110*, 087205.
17. Macia, F.; Hernandez, J.M.; Tejada, J.; Datta, S.; Hill, S.; Lampropoulos, C.; Christou, G. Effects of quantum mechanics on the deflagration threshold in the molecular magnet Mn 12 acetate. *Phys. Rev. B* **2009**, *79*, 092403.
18. Barco, E.D.; Kent, A.D.; Hill, S.; North, J.M.; Dalal, N.S.; Rumberger, E.M.; Hendrickson, D.N.; Chakov, N.E.; Christou, G. Magnetic quantum tunneling in the single-molecule magnet Mn12-acetate. *J. Low Temp. Phys.* **2005**, *140*, 119.
19. Stamp, P.C.E. Tunnelling secrets extracted. *Nature* **1996**, *383*, 125.
20. Wernsdorfer, W.; Bhaduri, S.; Boskovic, C.; Christou, G.; Hendrickson, D.N. Spin-parity dependent tunneling of magnetization in single-molecule magnets. *Phys. Rev. B* **2002**, *65*, 180403.
21. Papatriantafyllopoulou, C.; Zartilas, S.; Manos, M.J.; Pichon, C.; Clérac, R.; Tasiopoulos, A.J. A single-chain magnet based on linear $[Mn^{III}_2Mn^{II}]$ units. *Chem. Commun.* **2014**, *50*, 14873.
22. Coulon, C.; Miyasaka, H.; Clérac, R. Single-Chain Magnets: Approach and Experimental Systems. *Struct. Bond.* **2006**, *122*, 163.
23. Wang, T.-T.; Ren, M.; Bao, S.-S.; Liu, B.; Pi, L.; Cai, Z.-S.; Zheng, Z.-H.; Xu, Z.-L.; Zheng, L.-M. Effect of Structural Isomerism on Magnetic Dynamics: From Single-Molecule Magnet to Single-Chain Magnet. *Inorg. Chem*. **2014**, *53*, 3117.
24. Wang, H.-N.; Meng, X.; Dong, L.-Z.; Chen, Y.; Li, S.-L.; Lan, Y.-Q. Coordination polymer-based conductive materials: Ionic conductivity vs. electronic conductivity. *J. Mater. Chem. A* **2019**, *7*, 24059.
25. Yue, Q.; Gao, E.-Q. Azide and carboxylate as simultaneous coupler for magnetic coordination polymers. *Coord. Chem. Rev*. **2019**, *382*, 1.
26. Hui, J.K.-H.; Kishida, H.; Ishiba, K.; Takemasu, K.; Morikawa, M.-A.; Kimizuka, N. Ferroelectric Coordination Polymers Self-Assembled from Mesogenic Zinc(II) Porphyrin and Dipolar Bridging Ligands. *Chem.–A Eur. J.* **2016**, *22*, 14213.
27. Eddaoudi, M.; Moler, D.B.; Li, H.; Chen, B.; Reineke, T.M.; O'Keefe, M.; Yaghi, O.M. Modular Chemistry: Secondary Building Units as a Basis for the Design of highly porous and Robust Metal–Organic Carboxylate Frameworks. *Acc. Chem. Res*. **2001**, *34*, 319.
28. Yan, S.; Feng, L.; Wang, K.; Pang, J.; Bosch, M.; Lollar, C.; Sun, Y.; Qin, J.; Wang, X.; Zhang, P.; et al. Stable Metal—Organic Frameworks: Design, Synthesis, and Applications. *Adv. Mater.* **2018**, *30*, 1704303.
29. Zhou, H.-C.; Kitagawa, S. Metal-Organic Frameworks (MOFs). *Chem. Soc. Rev*. **2014**, *43*, 5415.

30. Ahmed, A.; Efthymiou, C.G.; Sanii, R.; Patyk-Kazmierczak, E.; Alsharabasy, A.M.; Winterlich, M.; Kumar, N.; Sensharma, D.; Tong, W.; Guerin, S.; et al. NUIG4: A biocompatible pcu metal–organic framework with an exceptional doxorubicin encapsulation capacity. *J. Mat. Chem. B* **2022**, *10*, 1378.
31. Winterlich, M.; Efthymiou, C.G.; Papawassiliou, W.; Carvalho, J.P.; Pell, A.J.; Mayans, J.; Escuer, A.; Carty, M.P.; McArdle, P.; Tylianakis, E.; et al. A biocompatible ZnNa 2-based metal–organic framework with high ibuprofen, nitric oxide and metal uptake capacity. *Mater. Adv*. **2020**, *1*, 2248.
32. Giménez-Marqués, M.; Hidalgo, T.; Serre, C.; Horcajada, P. Nanostructured metal–organic frameworks and their bio-related applications. *Coord. Chem. Rev*. **2016**, *307*, 342.
33. Mínguez Espallargas, G.; Coronado, E. Magnetic functionalities in MOFs: From the framework to the pore. *Coord. Chem. Rev*. **2018**, *47*, 533.
34. Li, H.; Wang, K.; Sun, Y.; Tollar, C.; Li, J.; Zhou, H.-C. Recent advances in gas storage and separation using metal–organic frameworks. *Mater. Today* **2018**, *21*, 108.
35. Xue, T.; Xu, C.; Wang, Y.; Wang, Y.; Tian, H.; Zhang, Y. Doxorubicin-loaded nanoscale metal–organic framework for tumor-targeting combined chemotherapy and chemodynamic therapy. *Biomater Sci.* **2019**, *7*, 4615.
36. Pascanu, V.; González Miera, G.; Ken Inge, A.; Martín-Matute, B. Metal–Organic Frameworks as Catalysts for Organic Synthesis: A Critical Perspective. *J. Am. Chem. Soc*. **2019**, *141*, 7223.
37. Li, H.; Li, L.; Lin, R.-B.; Zhou, W.; Zhang, Z.; Xiang, S.; Chen, B. Porous metal-organic frameworks for gas storage and separation: Status and challenges. *EnergyChem* **2019**, *1*, 100006.
38. Singh, N.; Singh, U.P.; Butcher, R.J. Luminescent sulfonate coordination polymers: Synthesis, structural analysis and selective sensing of nitroaromatic compounds. *Cryst. Eng. Comm*. **2017**, *19*, 7009.
39. Milios, C.J.; Stamatatos, T.C.; Perlepes, S.P. The coordination chemistry of pyridyl oximes. *Polyhedron* **2006**, *25*, 134.
40. Papatriantafyllopoulou, C.; Jones, L.F.; Nguyen, T.D.; Matamoros-Salvador, N.; Cunha-Silva, L.; Paz, F.A.A.; Rocha, J.; Evangelisti, M.; Brechin, E.K.; Perlepes, S.P. Using pyridine amidoximes in 3d-metal cluster chemistry: A novel ferromagnetic Ni12 complex from the use of pyridine-2-amidoxime. *Dalton Trans.* **2008**, *24*, 3153.
41. Efthymiou, C.G.; Cunha-Silva, L.; Perlepes, S.P.; Brechin, E.K.; Inglis, R.; Evangelisti, M.; Papatriantafyllopoulou, C. In search of molecules displaying ferromagnetic exchange: Multiple-decker Ni_{12} and Ni_{16} complexes from the use of pyridine-2-amidoxime. *Dalton Trans*. **2016**, *43*, 17409.
42. Papatriantafyllopoulou, C.; Stamatatos, T.C.; Efthymiou, C.G.; Cunha-Silva, L.; Almeida Paz, F.A.; Perlepes, S.P.; Christou, G. A High-Nuclearity 3d/4f Metal Oxime Cluster: An Unusual Ni_8Dy_8 "Core-Shell" Complex from the Use of 2-Pyridinealdoxime. *Inorg. Chem*. **2010**, *49*, 9743.
43. Nguyen, T.N.; Wernsdorfer, W.; Shiddiq, M.; Abboud, K.A.; Hill, S.; Christou, G. Supramolecular aggregates of single-molecule magnets: Exchange-biased quantum tunneling of magnetization in a rectangular $[Mn_3]_4$ tetramer. *Chem. Sci*. **2016**, *7*, 1156.
44. Ghosh, T.; Abboud, K.A.; Christou, G. New $Mn^{II}Mn^{III}_8$ and $Mn^{II}_2Mn^{III}_{10}Mn^{IV}_2$ clusters from the reaction of methyl 2-pyridyl ketone oxime with $[Mn_{12}O_{12}(O_2CR)_{16}(H_2O)_4]$. *Polyhedron* **2019**, *173*, 114145.
45. Stamatatos, T.C.; Foguet-Albiol, D.; Stoumpos, C.C.; Raptopoulou, C.P.; Terzis, A.; Wernsdorfer, W.; Perlepes, S.P.; Christou, G. New Mn_3 structural motifs in manganese single-molecule magnetism from the use of 2-pyridyloximate ligands. *Polyhedron* **2007**, *26*, 2165.
46. Mowson, A.M.; Nguyen, T.N.; Abboud, K.A.; Christou, G. Dimeric and tetrameric supramolecular aggregates of single-molecule magnets via carboxylate substitution. *Inorg. Chem*. **2013**, *52*, 12320.
47. Polyzou, C.D.; Efthymiou, C.G.; Escuer, A.; Cunha-Silva, L.; Papatriantafyllopoulou, C.; Perlepes, S.P. In search of 3d/4f-metal single-molecule magnets: Nickel(II)/lanthanide(III) coordination clusters. *Pure Appl. Chem*. **2013**, *85*, 315.
48. Efthymiou, C.G.; Mylonas-Margaritis, I.; Das Gupta, S.; Tasiopoulos, A.J.; Nastopoulos, V.; Christou, G.; Perlepes, S.P.; Papatriantafyllopoulou, C. Synthesis and characterisation of new Ni_2Mn, Ni_2Mn_2 and Mn_8 clusters by the use of 2-pyridyl oximes. *Polyhedron* **2019**, *171*, 330.
49. Nguyen, T.N.; Shiddiq, M.; Ghosh, T.; Abboud, K.A.; Hill, S.; Christou, G. Covalently Linked Dimer of Mn_3 Single-Molecule Magnets and Retention of Its Structure and Quantum Properties in Solution. *J. Am. Chem. Soc*. **2015**, *137*, 7160.
50. Mylonas-Margaritis, I.; Winterlich, M.; Efthymiou, C.G.; Lazarides, T.; McArdle, P.; Papatriantafyllopoulou, C. New insights into oximic ligands: Synthesis and characterization of 1D chains by the use of pyridine 2-amidoxime and polycarboxylates. *Polyhedron* **2018**, *151*, 360.
51. Mylonas-Margaritis, I.; Mayans, J.; McArdle, P.; Papatriantafyllopoulou, C. *Molecules* **2021**, *26*, 491.
52. Mylonas-Margaritis, I.; Gérard, A.; Skordi, K.; Mayans, J.; Tasiopoulos, A.; McArdle, P.; Papatriantafyllopoulou, C. From 1D Coordination Polymers to Metal Organic Frameworks by the Use of 2-Pyridyl Oximes. *Materials* **2020**, *13*, 4084.
53. Zhou, L.; Fan, H.; Zhou, B.; Cui, Z.; Qin, B.; Zhang, X.; Li, W.; Zhang, J. Tetranuclear cobalt (ii)—isonicotinic acid frameworks: Selective CO 2 capture, magnetic properties, and derived "Co 3 O 4" exhibiting high performance in lithium ion batteries. *Dalton Trans.* **2019**, *48*, 296.
54. Chen, D.M.; Zhang, N.N.; Liu, C.S.; Jiang, Z.H.; Wang, X.D.; Du, M. A Mixed-cluster approach for building a highly porous cobalt (II) isonicotinic acid framework: Gas sorption properties and computational analyses. *Inorg. Chem.* **2017**, *56*, 2379.
55. Wang, S.M.; Shivanna, M.; Yang, Q.Y. Nickel-Based Metal-Organic Frameworks for coal-bed Methane Purification with Record CH4/N2 Selectivity. *Angew. Chem.* **2022**, *134*, e202201017.

56. Xiao, Y.-F.; Wang, T.-T.; Zeng, H.-P. Synthesis, crystal structure and optical property of two zinc metal organic frameworks constructed from isonicotinic acid. *J. Mol. Struct.* **2014**, *1074*, 330.
57. Hu, H.; Chen, F.; Zhang, Z.; Liu, D.; Liang, Y.; Chen, Z. Heterometallic Metal-Organic Framework Based on [Cu4I4] and [Hf6O8] Clusters for Adsorption of Iodine. *Front. Chem.* **2022**, *10*, 864131.
58. Shi, G.; Xu, W.; Wang, J.; Yuan, Y.; Chaemchuen, S.; Verpoort, F. A Cu-based MOF for the effective carboxylation of terminal alkynes with CO2 under mild conditions. *J. CO2 Util.* **2020**, *39*, 101177.
59. Etaiw, S.E.H.; Fayed, T.A.; El-Bendary, M.M.; Marie, H. Three-dimensional coordination polymers based on trimethyltin cation with nicotinic and isonicotinic acids as anticancer agents. *Appl. Organomet. Chem.* **2018**, *32*, e4066.
60. Yang, Q.; Zhao, J.P.; Hu, B.W.; Zhang, X.F.; Bu, X.H. New Manganese (II) azido coordination polymers with nicotinic/isonicotinic acids as coligands: Synthesis, structure, and magnetic properties. *Inorg. Chem.* **2010**, *49*, 3746.
61. Zhang, Y.; Karatchevtseva, I.; Price, J.R.; Aharonovich, I.; Kadi, F.; Lumpkin, G.R.; Li, F. Uranium (VI) complexes with isonicotinic acid: From monomer to 2D polymer with unique U–N bonding. *RSC Adv.* **2015**, *5*, 33249.
62. Xu, W.; Zhang, C.J.; Wang, H.; Wang, Y. Two novel two-dimensional lanthanide (III) coordination polymers constructed from isonicotinic acid and iminodiacetic acid: Synthesis, structure, and luminescence properties. *J. Clust. Sci.* **2017**, *28*, 2005.
63. Xie, W.P.; Lu, L.P.; Feng, S.B.; Ran, X.R.; Gao, J.Y.; Chen, C.J.; Yue, S.T.; Cai, Y.P. 3D Heterometallic 3d–4f coordination polymers based on organodisulfonate ligand with isonicotinic acid as a co-ligand: Synthesis, crystal structures, photoluminescent and magnetic properties. *J. Coord. Chem.* **2015**, *68*, 1776.
64. Marandi, F.; Pantenburg, I.; Meyer, G. A new 3D coordination polymer of bismuth with nicotinic acid N-oxide. *J. Chem.* **2013**, *2013*, 845810.
65. Kang, M.; Yoon, S.; Ga, S.; Kang, D.W.; Han, S.; Choe, J.H.; Kim, H.; Kim, D.W.; Chung, Y.G.; Hong, C.S. High-Throughput Discovery of Ni (IN) 2 for Ethane/Ethylene Separation. *Adv. Sci.* **2021**, *8*, 2004940.
66. Bentiss, F.; Roussel, P.; Drache, M.; Conflant, P.; Lagrenée, M.; Wignacourt, J.P. Thermal evolution and crystal structure of a polymeric complex: Pb3 (3, 5-dicarboxylatopyrazole) 2 (NO3) 2· 4H2O. *J. Mol. Struct.* **2004**, *707*, 63.
67. Demir, S.; Çepni, H.M.; Hołyńska, M.; Kavanoz, M. A tetranuclear copper (II) complex with pyrazole-3, 5-dicarboxylate ligands: Synthesis, characterization and electrochemical properties. *Z. Für Nat. B* **2016**, *71*, 305.
68. King, P.; Clérac, R.; Anson, C.E.; Powell, A.K. The building block approach to extended solids: 3, 5-pyrazoledicarboxylate coordination compounds of increasing dimensionality. *Dalton Trans.* **2004**, *6*, 852.
69. Sen, R.; Saha, D.; Koner, S. Controlled Construction of Metal–Organic Frameworks: Hydrothermal Synthesis, X-ray Structure, and Heterogeneous Catalytic Study. *Chem. Eur. J.* **2012**, *18*, 5979.
70. Chandrasekhar, V.; Thirumoorthi, R. Reactions of 3, 5-pyrazoledicarboxylic acid with organotin chlorides and oxides. Coordination polymers containing organotin macrocycles. *Organometallics* **2009**, *28*, 2096.
71. Zhou, Y.H.; Wang, Z.Y. Four New Metal–Organic Supramolecular Networks Based on Aromatic Acid and Flexible Bis (imidazole) Ligand: Synthesis, Structures and Luminescent Properties. *J. Inorg. Organomet. Polym. Mater.* **2016**, *26*, 648.
72. Wang, M.; He, L.; Lin, Q. Dimension-related magnetism in heterometallic complexes based on the same [LnCu (dicarboxylpyrazole) 2] building moieties. *J. Solid State Chem.* **2018**, *265*, 29.
73. Wang, Y.; Li, X.X.; Jiang, H.; Xia, B.W.; Deng, N.; Zhu, Y.W.; Jin, G.P.; Ni, X.M.; He, J.B. Two new 2p–3d–4f heterometallic coordination polymers based on 3, 5-pyrazoledicarboxylic acid: Synthesis, crystal structures and magnetic properties. *Inorg. Chem. Commun.* **2013**, *35*, 34.
74. Liu, C.B.; Liu, L.; Wang, S.S.; Li, X.Y.; Che, G.B.; Zhao, H.; Xu, Z.L. Hydrothermal Syntheses and Crystal Structures of Three Zn (II) Coordination Compounds Constructed with 3, 5-Pyrazoledicarboxylic Acid. *J. Inorg. Organomet. Polym. Mater.* **2012**, *22*, 1370.
75. Yang, T.H.; Silva, A.R.; Shi, F.N. Six new 3d–4f heterometallic coordination polymers constructed from pyrazole-bridged $Cu^{II}Ln^{III}$ dinuclear units. *Dalton Trans.* **2013**, *42*, 13997.
76. Zhao, M.-Y.; Zhu, J.-N.; Li, P.; Li, W.; Cai, T.; Cheng, F.-F.; Xiong, W.-W. Structural variation of transition metal–organic frameworks using deep eutectic solvents with different hydrogen bond donors. *Dalton Trans.* **2019**, *48*, 10199.
77. Barman, S.; Furukawa, H.; Blacque, O.; Venkatesan, K.; Yaghi, O.M.; Jin, G.-X.; Berke, H. Incorporation of active metal sites in MOFs via in situ generated ligand deficient metal–linker complexes. *Chem. Commun.* **2011**, *47*, 11882.
78. Klongdee, F.; Boonmak, J.; Moubaraki, B.; Murray, K.S.; Youngme, S. Copper (II) coordination polymers containing neutral trinuclear or anionic dinuclear building units based on pyrazole-3, 5-dicarboxylate: Synthesis, structures and magnetic properties. *Polyhedron* **2017**, *126*, 8.
79. Wang, Y.; Song, Y.; Pan, Z.R.; Shen, Y.Z.; Hu, Z.; Guo, Z.J.; Zheng, H.G. Unprecedented Na I–Cu II–Ln III heterometallic coordination polymers based on 3, 5-pyrazoledicarboxylate with both infinite cationic and anionic chains. *Dalton Trans.* **2008**, *41*, 5588.
80. Zangl, A.; Klüfers, P.; Schaniel, D.; Woike, T. Photoinduced linkage isomerism of binuclear bis (pyrazole-3, 5-dicarboxylato)-bridged {RuNO} 6 centres. *Inorg. Chem. Commun.* **2009**, *12*, 1064.
81. Liu, C.B.; Ferreira, R.A.S.; Paz, F.A.; Cadiau, A.; Carlos, L.D.; Fu, L.S.; Rocha, J.; Shi, F.N. Highly emissive Zn–Ln metal–organic frameworks with an unusual 3D inorganic subnetwork. *Chem. Commun.* **2012**, *48*, 7964.
82. Fa-Nian, S.H.I.; Silva, A.R.; Yang, T.H.; Rocha, J. Mixed Cu (ii)—Bi (iii) metal organic framework with a 2D inorganic subnetwork and its catalytic activity. *CrystEngComm* **2013**, *15*, 3776.

83. Tian, J.L.; Yan, S.P.; Liao, D.Z.; Jiang, Z.H.; Cheng, P. Syntheses, structures and properties of two one-dimensional chain complexes:[Mn (Hpdc)(H2O) 2] n and [Cu2 (Hpdc) 2][4, 4′-dpdo](Hpdc= 3, 5-pyrazoledicarboxylic acid group, dpdo = 4, 4′-dipyridyl-N, N′-dioxide hydrate). *Inorg. Chem. Commun.* **2003**, *6*, 1025.
84. Driessen, W.L.; Chang, L.; Finazzo, C.; Gorter, S.; Rehorst, D.; Reedijk, J.; Lutz, M.; Spek, A.L. Two pyrazolato-bridged, linear trinuclear Cu (II) complexes. Crystal structures and magnetic properties. *Inorg. Chim. Acta* **2003**, *350*, 25.
85. King, P.; Clerac, R.; Anson, C.E.; Coulon, C.; Powell, A.K. Antiferromagnetic three-dimensional order induced by carboxylate bridges in a two-dimensional network of [Cu3 (dcp) 2 (H2O) 4] trimers. *Inorg. Chem.* **2003**, *42*, 3492.
86. Addison, A.W.; Rao, T.N.; Reedijk, J.; van Rijn, J.; Verschoor, G.C. Synthesis, structure, and spectroscopic properties of copper(II) compounds containing nitrogen–sulphur donor ligands; the crystal and molecular structure of aqua [1,7-bis(N-methylbenzimidazol-2′-yl)-2,6-dithiaheptane]copper(II) perchlorate. *J. Chem. Soc. Dalton Trans.* **1984**, *7*, 1346.
87. Chilton, N.F.; Anderson, R.P.; Turner, L.D.; Soncini, A.; Murray, K.S. PHI: A powerful new program for the analysis of anisotropic monomeric and exchange-coupled polynuclear d-and f-block complexes. *J. Comput. Chem*. **2013**, *34*, 1164.
88. Bernasek, E. Pyridineamidoximes. *J. Org. Chem.* **1957**, *22*, 1263.
89. Orama, M.; Saarinen, H.; Korvenranta, J. Formation of trinuclear copper(II) complexes with three pyridine oxime ligands in aqueous solution. *J. Coord. Chem*. **1990**, *22*, 183.
90. Sheldrick, G.M. SHELXT—Integrated space-group and crystal-structure determination. *Acta Crystallogr. Sect. A Found. Adv.* **2015**, *71*, 3.
91. McArdle, P.; Gilligan, K.; Cunningham, D.; Dark, R.; Mahon, M. A method for the prediction of the crystal structure of ionic organic compounds—The crystal structures of o-toluidinium chloride and bromide and polymorphism of bicifadine hydrochloride. *Cryst. Eng. Comm*. **2004**, *6*, 303.
92. Brandenburg, K.; Putz, H. *DIAMOND, Version 2003.2001d*; Crystal Impact GbR: Bonn, Germany, 2006.